Fiber trapping in low-consistency refining: new parameters to describe the refining process

TOM LUNDIN, WARREN BATCHELOR, AND PEDRO FARDIM

ABSTRACT: Fiber trapping in refining has been defined by the fraction *f* of the bar edges that trap fibers as they cross, and by the number of fibers *i* trapped under each section of bar. From these parameters, equations were derived to calculate the number of impacts that a fiber undergoes during refining and the maximum force experienced during each impact. Refiner power versus gap was measured for a conical laboratory refiner at maximum peripheral speeds ranging from 4 m/s to 27 m/s and consistencies ranging from 1% to 6% for one softwood kraft pulp. The data were used to calculate relative changes in *i* and *f* as a function of consistency and speed. It was found that *f* was extremely sensitive both to an increase in refiner rotational speed and to a reduction in pulp consistency. A reduction in consistency from 4% to 2% at 20 m/s (3000 rpm) led to a decrease in the trapping fraction, *f*, by approximately 80%. The number of fibers trapped under each section of bar also decreased, although to a lesser extent. The reduction in fiber trapping greatly increased the forces on the fibers, leading to enhanced fiber shortening and reduced refining efficiency.

Application: Fiber trapping is a hidden variable affecting refining efficiency. This paper describes how to estimate relative changes in fiber trapping and shows how fiber trapping impacts the refining process.

Low-consistency refining is the principal treatment for altering the mechanical properties of paper made from chemical pulps. A pulp refiner changes fiber structure by trapping fiber mats between rotor and stator bars and mechanically treating them to achieve plastic deformation of the fibers. Three separate forces are imposed by refiner bars on the fibers [1-3]: a normal force compressing the fiber mat, a shear force generated by the bar surface moving over the compressed mat of fibers, and a corner force exerted at the edges of the bars.

Refiners are characterized on an energy basis by the specific energy consumption (*SEC*), which is the energy per unit mass of pulp, and by a measure of refining intensity. Measures of refining intensity can be categorized by whether they consider fiber trapping. Examples of the first category include the widely used specific edge load (*SEL*) [4] as well as the specific-surface-load theory [5]. These measures of intensity always assume that when bars cross, fibers will be trapped. Other approaches [6,7] do consider fiber trapping, but only as the ratio of fiber dimensions to groove dimensions. In the C-factor [7], the probability of trapping is given as $l/(l+D)$, where l is the fiber length and D is the groove depth. This expression represents the probability that a given fiber will come into contact with a rotor bar as it crosses a groove. Implicit here is the assumption that if the fiber comes into contact with the bar, then it will be trapped. This probability does not consider bar-edge sharpness, even though this factor is indeed important [8-10]. The equation above predicts that the number of fiber layers trapped at any point will be proportional to consistency, because the number of fibers coming into contact with the bar will be proportional to consistency.

The authors previously developed a method to measure relative changes in fiber trapping indirectly by measuring power consumption as a function of refining gap [11]. In this paper, the authors develop refining equations that include the effect of fiber trapping, determined by measurements on softwood kraft pulp that show how fiber trapping is affected by consistency and speed, and how these changes in fiber trapping alter refining outcomes.

THEORY

The primary variable controlling refining is the specific energy consumption (*SEC*), given by Eq. 1:

$$SEC = \frac{tP_{net}}{C_F V} \quad \text{[closed loop/batch refining]}$$
$$= \frac{P_{net}}{C_F \dot{M}} \quad \text{[continuous flow refining]} \qquad (1)$$

where P_{net} is the net refiner power (kW) and C_F the pulp consistency (kg/m³). For closed-loop/batch refining, V is the total volume in the closed-loop system (including volume inside the refiner and volume inside the recirculation loop), and the total refining time is t. For continuous-flow refining, $\dot{M}$ is the mass flow rate through the refiner.

Refining is also characterized by specific edge load (*SEL*), which is given by Eq. 2:

$$SEL = \frac{P_{net}}{\omega CEL}\,, \tag{2}$$

where *CEL* is the cutting-edge length per revolution, projected in the radial direction, and ω is the rotational speed in revolutions per second. *SEL* is an empirical parameter which represents the energy transferred per bar crossing per unit length of rotor bar crossing over a unit length of stator bar [12].

The two factors that characterize the refiner action in trapping and treating fibers are the fraction *f* of the bar that traps fibers and the number of fibers *i* trapped under the bar edge at each point where a fiber mat is trapped. In the following work, these parameters are combined with the *SEC* and *SEL* as described above to characterize refining action on fibers, based on the maximum force applied to the fibers and the number of times this force is applied. This line of reasoning follows that originally developed by Kerekes for the C-factor [7] and later extended to a force-based characterization [12].

To trap a mat one fiber wide requires a refiner-bar segment length equal to the width of a fiber, d_w, when projected perpendicularly to the direction of bar motion. Refining-gap measurements indicate that fibers are processed as a mat. Therefore, for each fiber that is in contact with the rotor-bar edge, there will be a number of additional fibers underneath it. Not all bar edges will capture a fiber mat. Here the fraction of the bar that traps fibers will be designated as *f*, and the number of fiber layers in the mat at each point of trapping will be designated as *i*.

Figure 1 is a schematic diagram of this concept. This diagram shows a segment of rotor bar and of stator bar, each of length *x*. Fibers have been trapped at five points along the bar, and at each of these points, three fibers have been trapped, for a total of fifteen fibers. From this diagram, $f = 5d_w/x$ and i=3.

The number of fibers per second in contact with the bar edges as they cross is $f\omega CEL/d_w$, and the total number of fibers that are impacted per second is $if\omega CEL/d_w$. The total number of fibers refined is:

$$\begin{aligned} &C_F\dot{M}/lw && \text{continuous flow (per s)} \\ &C_F V/lw && \text{closed loop/batch (total number)} \end{aligned} \tag{3}$$

where *l* is the fiber length and *w* is the fiber coarseness.

The number of impacts per fiber, N^*, is:

$$\begin{aligned} N^* &= (if\omega CEL/d_w)/(C_F\dot{M}/lw) && \text{continuous flow} \\ &= t(if\omega CEL/d_w)/(C_F V/lw\ ) && \text{closed loop/batch} \end{aligned} \tag{4}$$

Substituting Eqs. 1 and 2 into Eq. 4 and rearranging yields:

$$N^* = fi\frac{lw}{d_w}\frac{SEC}{SEL} \quad \text{for both modes} \tag{5}$$

The energy absorbed for one crossing per projected unit length of bar in contact with fibers is *SEL/f*. The factor *f* is necessary here because the *SEL* is an average energy over all bar surfaces, whether or not they have a fiber mat trapped. If the bars cross without trapping a fiber mat, then no energy will be absorbed at this point. Therefore the energy must be redistributed to the points along the bar that are covered with fibers. The energy absorbed in passage over a mat with the width of a single fiber is $d_w SEL/f$.

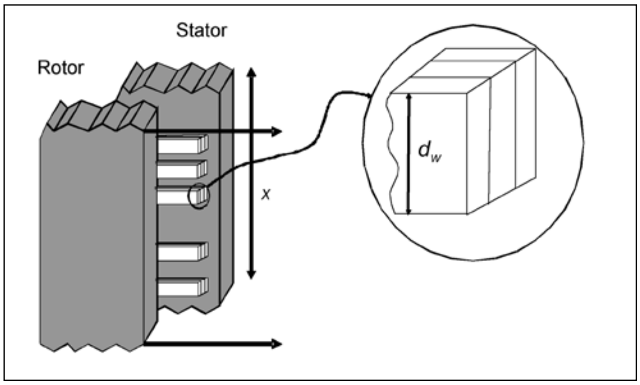

1. Schematic diagram showing three layers of fibers trapped at five positions along a bar of length x.

Refiner-bar force measurements [1,2,13] have shown that the work absorbed in a bar crossing can be divided into the work done by the bar edge to force the fibers into the gap between rotor and stator and the work required to slide the rotor-bar surface over the compressed fiber mat. For a given level of fiber-mat strain, the work done by the bar edge should be proportional to *i*. The sliding-force work will depend on the compressive force applied to the mat, the coefficient of friction, and the bar width, but will be independent of *i*. Recent measurements [13] have suggested that the amount of work performed by the bar edge is much greater than the sliding work, and therefore, to simplify the analysis, the sliding work has been ignored in the analysis that follows.

To determine the maximum shear force, F^s_{max}, applied to the fibers, it can be assumed that the shear force F^s_{max} required to form the mat and compress it to a given strain is proportional to the number of fibers trapped and to some function of the gap, Ω. Then it is possible to write:

$$F^s_{max} = id_w\Omega(g)\,, \tag{6}$$

If all the energy is consumed in working the fibers into the gap, then the force-distance curve will be triangular, acting over a distance of one fiber length with maximum shear force F^s_{max}. Then the work performed during passage over a mat of a single fiber width is $lF^s_{max}/2$. Because this work can also be written as $d_w SEL/f$, it is possible to state that:

$$F^s_{max} = 2d_w SEL/lf\,, \tag{7}$$

and combining Eqs. 6 and 7 gives:

$$P_{net} = \omega CEL\frac{2fi}{l}\Omega(g)\,. \tag{8}$$

The form of Ω (*g*) can be investigated by measuring refiner power as a function of refining gap. The authors have found that a negative exponential function satisfactorily fits the data for net power versus gap at different speeds and consistencies.

Assuming that $\Omega\,(g/i) = k\,\exp(-g/\tau)$, then:

$$P_{net} = \omega CEL \frac{2fi}{l} k \exp(-g/\tau) \quad . \tag{9}$$

Thus the data for P_{net} versus gap, when fitted with $P_{net} = c\exp(-g/g_t)$, produce two parameters: $c = 2k\omega CEL\,(fi/l)$ and τ.

The number of layers, i, in the fiber mat trapped under each section of bar will be proportional to the point at which the fiber mat first takes up load and begins to experience strain due to compressive forces; this point is defined as g_0. Fitting a negative exponential function to the data makes it difficult to define g_0 unambiguously, because a negative exponential function is equal to 0 only when $g = \infty$. This problem has already been solved by defining g_0 as the gap at the point where the fitted function is 1% above the no-load power [11]:

$$c\exp\left(-g/\tau\right) = 0.01\left(a + b\,g\right) \tag{10}$$

and solving numerically to determine g_0. In Eq. 10, a and b are fitting constants for the no-load power. If the fitted power at g_0 is defined as $P_0 = c\,\exp(-g_0/\tau)$, then: $g_0 = \tau\ln(c/P_0)$.

If there are two power curves, labeled as 1 and 2, which have been fitted with $P_{net} = c\,\exp(-g/g_t)$, then, provided the furnish is the same, the following ratios can be written:

$$\frac{i_1}{i_2} = \frac{g_o^1}{g_o^2} = \frac{\tau_1 \ln\left(c_1 / P_0^1\right)}{\tau_2 \ln\left(c_2 / P_0^2\right)} \tag{11}$$

and

$$\frac{f_1}{f_2} = \frac{c_1}{c_2} \frac{\omega_2 CEL_2 \tau_2 \ln\left(c_2 / P_0^2\right)}{\omega_1 CEL_1 \tau_1 \ln\left(c_1 / P_0^1\right)} \quad , \tag{12}$$

which for the same set of fillings simplifies to:

$$\frac{f_1}{f_2} = \frac{c_1}{c_2} \frac{\omega_2}{\omega_1} \frac{g_o^2}{g_o^1} \quad . \tag{13}$$

This enables calculation of bar coverage and mat thickness ratios for the two cases and of relative changes in forces and number of impacts on fibers as conditions change.

EXPERIMENTAL

In these experiments, researchers used a ProLab™ laboratory refining station supplied by Metso Paper. **Table I** shows the technical specifications of the refiner. The refiner was equipped with conical fillings of standard Long Medium (LM) type with an actual cutting-edge length (*CEL*) of 52 m/rev and bar and groove widths of 5 mm and 6 mm, respectively. The automated refiner handles softwood slurries of 2% to 7% consistency at a typical batch size of 50 L. The refiner was operated with the rotor revolving in the non-pumping direction. The rotor position is measured by an inductive linear position sensor from the rotor axial movement.

Parameter	Value
Power (kW)	30
Rotor diameter min-max (mm)	58–130
Pulp consistency (%)	2–7*
Pulp flow (L/min)	50–120
Pulp feeding pressure (bar)	0.5–6
Rotational speed (1/min)	600–4500
Peripheral speed, d_{min} (m/s)	1.8–13.7
Peripheral speed, d_{max} (m/s)	4.0–30.6
SEC/batch (kWh/t)	10–45*
SEL (J/m)	0.1–8*
SSL (J/m^2)	115–1500*

**depending on type of fillings and pulp*

I. Technical specifications of the ProLab™ refiner.

To determine the refining gap, the position where the fillings come into contact must be located. For this purpose researchers performed a zeroing procedure to determine the point of bar-to-bar contact while running the refiner dry at 1500 rpm. This position was determined by a specific vibration level of the fillings at their zero point. The refining gap was then calculated from the absolute linear rotor position by subtracting the zero value and accounting for the fillings' geometry. A limitation of this zeroing procedure is that the contact position has been found to vary from measurement to measurement, with a range of ±0.03 mm around the average.

A single zeroing procedure was performed before each consistency series (1%–6%). A separate batch of pulp was prepared for each trial that was performed at pulp consistencies of 1, 2, 3, 4, 5, and 6 weight-percent. At each pulp consistency, a refiner loading sequence (2-mm gap–minimum–2-mm gap) was performed consecutively at speeds of 4, 10, 15, 20, and 27 m/s (600, 1500, 2250, 3000, and 4000 rpm, respectively; rotor speeds measured at the largest rotor diameter).

The softwood ECF-bleached dry-lap kraft pulp was produced by a pulp mill in southeastern Finland. The reinforcement pulp had a length-weighted fiber length of 2.38 mm and an average fiber coarseness of 0.183 mg/m.

RESULTS AND DISCUSSION

The data obtained for the various conditions are shown in **Fig. 2,** sections A–D, except for the 2250-rpm data, which were similar to those obtained at 1500 rpm. These figures include the data as well as the negative exponential functions used to fit the data. Each data set shows the net refining power after subtraction of the no-load power using the method described in [11]. The data consistently show that a decrease in consistency reduces the net refining power at a given gap and speed.

Figure 3 shows the initial loading points, g_0, where the pulp mat between the bars first takes up load. The data in Fig. 2 show that the negative exponential function fits the

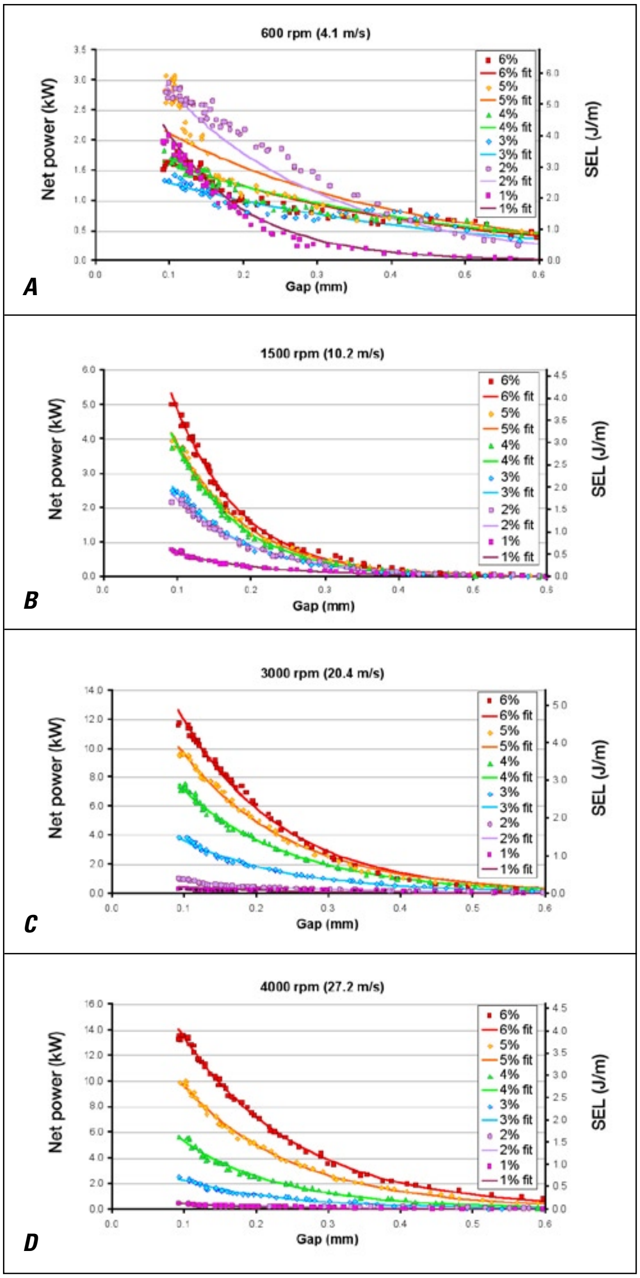

2. Refiner loadability determined at different rotational speeds and pulp consistencies (A: 600 rpm, B: 1500 rpm, C: 3000 rpm, and D: 4000 rpm).

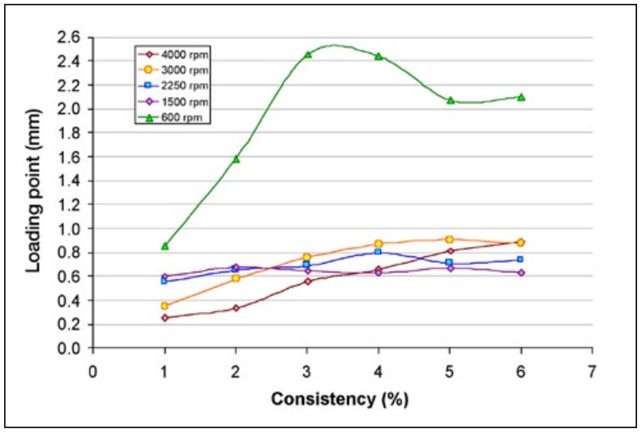

3. Refiner loading point, g_0, as a function of consistency at different rotational speeds.

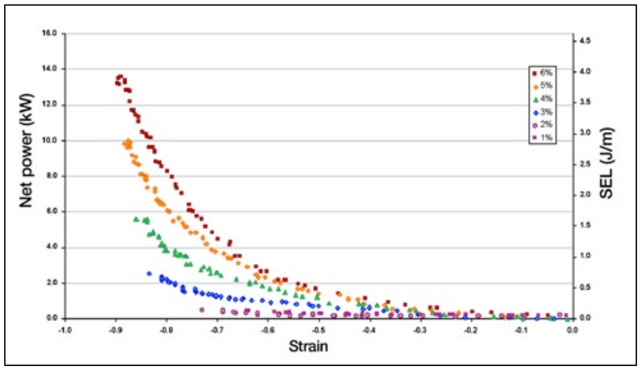

4. Fiber-mat compressive strain vs. refiner net power at different pulp consistencies and 4000 rpm (27 m/s).

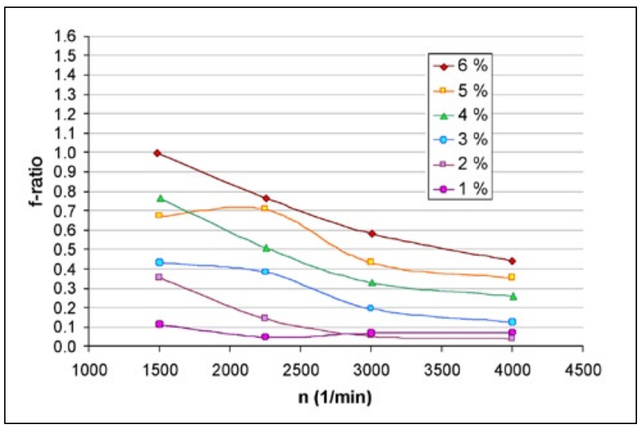

5. Relative changes in proportion of bar edges trapping fibers. 1.0= 1500 rpm at 6% consistency.

data excellently at all refiner speeds except 600 rpm, where all fits were poor except for that at 1% consistency. The g_0 values in Fig. 3 for the 600-rpm data were up to four times higher than for any other data sets. The anomalous data at 600 rpm were probably affected by fiber flocculation at the low peripheral bar speeds of 2–4 m/s. Because of the difficulties in making sense of these data, they were removed from further processing.

For a given furnish and level of refining, g_0 is proportional to the number of fiber layers i trapped between the bar surfaces. A higher pulp consistency generally provided a higher value of g_0 at the highest speeds of 3000 and 4000 rpm, while g_0 was essentially independent of consistency at the lower speeds (2250 and 1500 rpm). Below 2% consistency, a higher refiner speed resulted in a systematically smaller value of g_0.

The values of g_0 shown in Fig. 3 were used to convert the data in Fig. 2 to net power versus compressive strain curves, which are shown in **Fig. 4** for the 4000-rpm data. As consistency was reduced, the net power to operate the refiner at a given strain decreased sharply. The area of fiber mat compressed between the bars must have been reduced correspondingly.

The next step was to calculate how the fiber-trapping parameters change as a function of consistency and refiner speed. Eqs. 12 and 14 give ratios of f and i for refining the same pulp

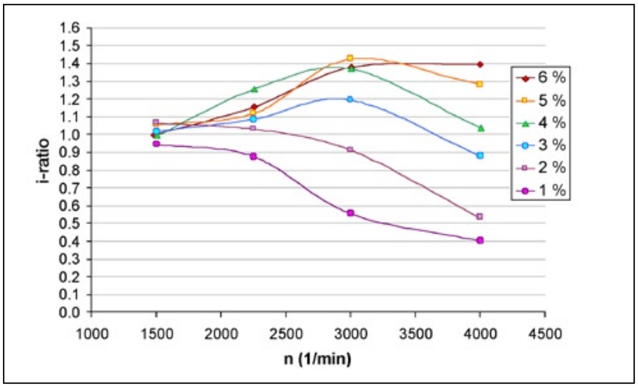

6. Relative changes in number of fiber layers trapped. 1.0= 1500 rpm at 6% consistency.

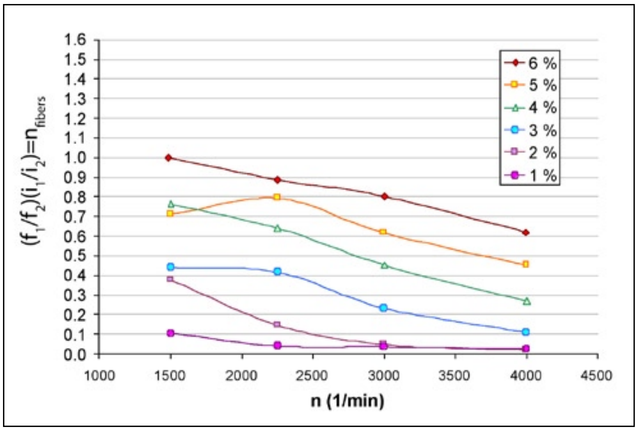

7. Relative change in total number of fibers, fi=n, trapped between refiner bars. 1.0= 1500 rpm at 6% consistency.

at different consistencies. To calculate these ratios, a reference point is needed. The authors chose the reference point with the highest level of fiber trapping (6% consistency and 1500 rpm), which was the slowest speed measured with a fully fluidized pulp, as well as the highest consistency. For all subsequent work, it was assumed that f=1 at this reference point.

The parameters from the negative exponential fits were used together with Eqs. 12 and 13 to calculate the relative changes in f, in i, and in the total number of fibers trapped ($f{\cdot}i$), which are shown in **Figs. 5**, **6**, and **7**, respectively.

A reduction in consistency or an increase in rotational speed both reduced the fraction f of bar edges that trapped fibers. The consistency effects can be understood as arising both from fewer fibers in the grooves available for capture and from a reduced number of fiber-fiber contacts for each fiber, which reduces the capacity to catch fibers as they come into contact with the bar edge, allowing them to be trapped between bar surfaces.

The relative thickness of the trapped fiber mat, determined as the i-ratios, was a function of both bar rotational speed and pulp consistency, although the variation was not as large as in f, as shown in Fig. 5. The thickness of the trapped fiber mat was more sensitive to pulp consistency at 3000 and 4000 rpm, cases in which a decreased consistency resulted in the trapping of a thinner fiber mat. At 1500 and 2250 rpm, the fiber-mat thickness was almost independent of consistency. The data for the relative number of fibers trapped (7) were dominated by the change in f, showing similar trends to those shown in Fig. 5.

The work so far has shown how relative changes in fiber-trapping behavior can be estimated from refiner loadability measurements. To complete the picture, it must be shown that changes in fiber trapping also produce changes in the outcome of refining.

The two parameters that characterize refining action are the number of impacts per fiber, N^* (Eq. 6), and the maximum shear force applied in each impact $F^s_{\max}$, (Eq. 8). These equations require the fiber length, l, coarseness, w, and width, d_w, as well as f and i. Fiber length and coarseness were measured using a FiberLab® analyzer. The average Kajaani fiber width was 28.5 µm, independently of the level of refining. Assuming that the cross-sections of the fibers are approximately circular or square will give a fiber thickness of 28.5 µm.

To determine i, it is assumed that the fiber mat first takes up load when all the spaces between the fibers have been removed, i.e., when:

$$i = g_o / d_w \quad . \tag{14}$$

This is likely to be an upper bound. The final variable required is f, which after normalization was plotted in Fig. 5. There is no way of determining the value of f at the reference point, so instead the assumption is made that the reference point (6% and 1500 rpm) has f=1, as an upper-bound case. The data in Fig. 5 then give the value of f at all other speeds and consistencies. For this pulp, Eqs. 6 and 8 then become Eqs. 15 and 16, respectively:

$$N^* = fg_o \frac{lw}{d_w^2} \frac{SEC}{SEL} = 2.479x10^{-4} f \frac{SEC}{SEL} \ , \tag{15}$$

$$F_{\max} = 2d_w SEL / lf = 0.0234\, SEL / f \quad . \tag{16}$$

rpm (1/min)	Bar velocity[a] (m/s)	Consistency (weight%)	SEL[b] (J/m)	g_0 (mm)	f (-)	F_{max}[c] (N)	N^*[c] (pcs)	l(w)[c] (mm)
3000	10.2-20.4	4	3.84	0.874	0.332	0.3282	51.94	2.02
3000	10.2-20.4	4	0.94	0.874	0.322	0.0628	257.86	2.43
3000	10.2-20.4	2	1.89	0.583	0.056	0.9593	11.54	2.18
3000	10.2-20.4	2	0.63	0.583	0.056	0.3313	32.53	1.93

[a] lower value at smaller cone diameter and higher value at larger cone diameter; [b] average value during refining trial; [c] value at the SEC level of circa 400 kWh/t

II. Variation in estimated fiber-trapping parameters with applied refining conditions. It is assumed that f=1 at 1500 rpm.

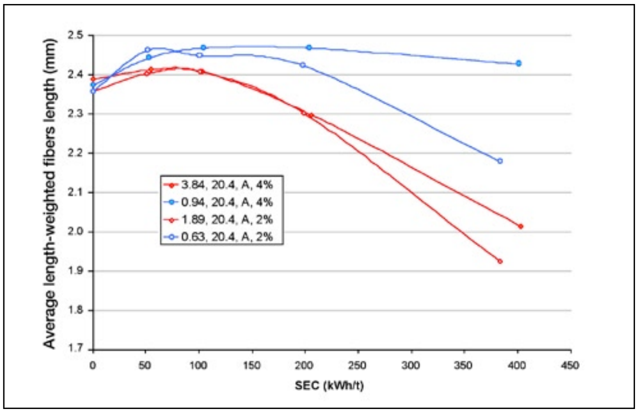

8. *Fiber length development during refining of the ECF$_2$ pulp at 3000 rpm. Labels indicate SEL (J/m), rotor peripheral speed at larger end (m/s), fillings code and pulp consistency.*

For refining at *SEL*=2 J/m to a SEC of 100 kWh/t with *f*=1, Eqs. 15 and 16 predict that each fiber will have experienced 49.5 impacts with a maximum shear force of 0.047 N. These estimates appear reasonable and in line with estimates in the literature. For example, a recent force estimate from a very different theoretical construction yielded a maximum shear force of 0.034 N under similar refining conditions [12]. Given the complexities and unknowns of the situation, the close agreement between these two estimates is encouraging. Eqs. 15 and 16 predict that halving *f* will halve the number of contacts and double the maximum force, which should greatly increase fiber shortening. Next, fiber length development at different pulp consistencies, refiner speeds, and SEL values was compared in four trials to show that a change in fiber trapping has a measurable influence on refining outcomes. The data are shown in **Fig. 8** and the corresponding fiber-trapping parameters in **Table II**.

During the refining trials, conditions of 4%, 3000 rpm, and SEL 3.8 J/m resulted in substantial fiber shortening. At 2%, the refiner could not apply more than 1.9 J/m to the fibers without clashing. This was, however, not the case at 1500 rpm, when 3.8 J/m could be applied. Calculation of the fiber-trapping parameters gives an explanation for this behavior: the maximum force applied to the trapped fibers at 2% and 1.9 J/m was three times as great as at 4% and 3.8 J/m, because *f* at 2% consistency was only approximately one-fifth of the corresponding value when refining at 4% consistency. Therefore, the fibers were more severely shortened, despite the lower *nominal* SEL.

The greatest force estimated (Table II) was 0.96 N—well above measured values of single-fiber breaking loads. One possible reason for this is that the theory assumes that all energy is consumed by working fibers into the gap and none is consumed by sliding the rotor bar across the compressed fiber mat. Single-bar refiner measurements [1,2,12] show that both components exist. Therefore, neglecting the energy consumed in sliding the rotor-bar surface over the compressed mat will overestimate the energy consumed in trapping the fibers, thus overestimating the maximum shear force. Lateral compressions of single pulp fibers have revealed a two-stage deformation: initial lumen collapse under low load and high strain, followed by cell-wall compression but lower additional strain at much higher load [14]. During repeated load cycling of single pulp fibers, the most significant changes in transverse modulus and mechanical loss coefficient were reported to occur during the first 5–10 loadings [15]. Studies on transverse compression of single kraft pulp fibers [16] yielded compression curves (fiber thickness vs. force) comparable to some of the power-gap relationships observed in this work.

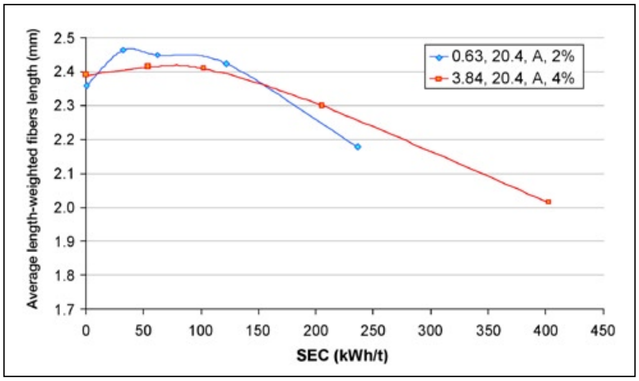

9. *Comparison of fiber length development at SEL of 3.84 J/m at 4% consistency and at SEL of 0.63 J/m at 2% consistency. The SEC values used for 2% consistency have been scaled by 32/52.*

It is also very interesting to compare fiber length development for the two trials in cases where the forces on the fibers are the approximately the same, i.e., with 4% consistency at 3.84 J/m and with 2% consistency at 0.63 J/m. Despite the similarity in forces, the data in Fig. 8 show that fiber length is reduced more slowly at 0.63 J/m and 2%. The reason can be seen in Table II; the estimated number of impacts at 3.84 J/m and 4% was 52, while at 0.63 J/m and 2%, the number of impacts per fiber was only 32. Thus the development of fiber length for the 2% trial at 0.63 J/m should be similar to the data at 4% consistency and a *SEL* of 3.83 J/m, provided that the *SEC* is decreased by a factor of 32/52. This proposition is tested in **Fig. 9**, which compares fiber length development in the two cases; the *SEC* for the 0.63 J/m and 2% consistency trial has been corrected by a factor of 32/52 to reflect the reduction in the number of impacts per unit of refining energy.

The data show that when the 2% data are corrected for the number of impacts, the observed fiber length development is approximately the same. Thus, fiber trapping can impact the efficiency of refining both by changing the force that is applied to the fibers and by changing the number of impacts, for refining at the same nominal conditions.

CONCLUSIONS

Fiber trapping was characterized by the fraction of the bar edge, *f*, that traps fibers and the number of fiber layers, *i*, at each point where a fiber mat is trapped. The authors developed equations to estimate relative changes in fiber-trapping behavior from refiner loadability measurements. Reducing refining consistency or increasing refiner rotational speed both reduced *f*. The relative thickness of the trapped fiber mat, determined as the i-ratios, also decreased with higher rotational speed or lower consistency, although the variation was small. The thickness of the trapped fiber mat was more sensitive to pulp consistency at the higher rotational speeds (3000 and 4000 rpm), where a decrease in pulp consistency resulted in the trapping of a thinner fiber mat. At 1500 and 2250 rpm, the fiber-mat thickness was almost independent of pulp consistency. The data for the relative number of fibers trapped were dominated by the change in f. From the theory, estimates were derived for the maximum force and the number of impacts. A reduction in consistency from 4% to 2% at 3000 rpm was found to reduce the bar trapping fraction, f, by approximately 80%. The number of fibers trapped under each section of bar also decreased, although to a lesser extent. The reduction in fiber trapping greatly increased the forces on the fibers, increasing fiber shortening and reducing the efficiency of the refining process. **TJ**

ACKNOWLEDGEMENTS

The Research Institute of the Åbo Akademi Foundation and the Finnish Ministry of Education through the International Doctoral Program in Pulp and Paper Science and Technology (PAPSAT) are acknowledged for financial support. Metso Paper is acknowledged for providing the advanced laboratory refining equipment.

Received: February 19, 2007
Revised: January 17, 2008
Accepted: January 21, 2008

LITERATURE CITED

1. Batchelor, W.J., Martinez, D.M., Kerekes, R.J., et al., *J. Pulp Paper Sci.* 23(1): J 40(1997).
2. Martinez, D.M., Batchelor, W.J., Kerekes, R.J., et al., *J. Pulp Paper Sci.* 23(1): J 11(1997).
3. Batchelor, W. and Ouellet, D., *Proceedings, 4th International Refining Conference*, PIRA International, Leatherhead, U.K., 1997, Paper 2.
4. Brecht, W., *Tappi* 50(8): 40A(1967).
5. Lumiainen, J., *Pulp and Paper International* 32(8): 46(1990).
6. Leider, P.J. and Nissan, A.H., *Tappi* 60(10): 85(1977).
7. Kerekes, R.J., *Nordic Pulp Paper Res. J.* 5(1): 3(1990).
8. Ebeling, K., *Symposium on Fundamental Concepts of Refining*, IPC, Appleton, WI, 1980, p. 1.
9. Rihs, J., *3rd International Refining Conference*, PIRA International, Leatherhead, U.K., 1995, Paper 10.
10. Berger, T.H., *Proceedings, 4th International Refining Conference*, PIRA International, Leatherhead, U.K., 1997, Paper 18.
11. Batchelor, W.J., Lundin, T., and Fardim, P., *TAPPI J.* 5(8): 31(2006).
12. Kerekes, R.J. and Senger, J.J., *Journal of Pulp and Paper Science* 32(1): 1(2006).
13. Senger, J., Siadat, A., Ouellet, D., et al., *Journal of Pulp and Paper Science* 30(9): 247(2004).
14. Hartler, N. and Nyren, J., *Tappi Special Technical Association Publication* 8: 265–277 (1970).
15. Dunford, J.A. and Wild, P.M., *J. Pulp Paper Sci.* 28(4): 136(2002).
16. Wild, P., Omholt, I., Steinke, D., et al., *Journal of Pulp and Paper Science* 31(3): 116(2005).

INSIGHTS FROM THE AUTHORS

Our conventional low consistency refining technology with barred devices dates back about 340 years. The topic has been researched from numerous angles, but seldom from a fiber-point-of-view that might reveal something new about the mechanisms behind the fiber treatment occurring between refiner bars.

Our previously published method introduced a new way of quantifying the trapping of pulp fibers by refiner bars. In this work, we extended the theory to calculate the number and size of the impacts an average fiber experiences. We discovered that the bar coverage was greatly dependent on bar velocity and pulp consistency, which both are key factors in the process. Previous research has not specifically considered bar coverage. We experienced initial difficulties due to scatter in data, but we solved this mathematically.

One key finding was that the bar coverage of trapped fibers is very sensitive to pulp consistency for the reinforcement pulp we tested. Hence, refining at high speed and small consistency led to reduced fiber trapping by bars that reduced process efficiency and supplied greater forces on the fibers leading to an inferior fiber treatment.

One way mills can use this work is to realize that they might pay more attention to controlling consistency during refining. If consistency changes affect the bar coverage, then *SEL* cannot be considered a sufficient control parameter, since a change in bar coverage affects the harshness of the fiber treatment significantly, even when the nominal refining intensity (*SEL*) has been kept constant.

The next step for this work is to apply our method to hardwood pulp data for elucidating their fiber trapping behavior.


Lundin


Fardim


Batchelor

Tom Lundin is a researcher and Pedro Fardim a professor in the Laboratory of Fiber and Cellulose Technology, Åbo Akademi University, Turku/Åbo, Finland. Contact Lundin at tom.lundin@abo.fi. Warren Batchelor is a senior lecturer at the Australian Pulp and Paper Institute, Monash University, Melbourne, Australia.